Available online at www.sciencedirect.com
SCIENCE DIRECT®
International Journal of Heat and Mass Transfer 47 (2004) 757–773
International Journal of HEAT and MASS TRANSFER
www.elsevier.com/locate/ijhmt

Effects of a flow disturbing plate on pool boiling heat transfer

Myeong-Gie Kang *

Department of Mechanical Engineering Education, Andong National University, 388 Songchun-dong, Andong-city, Kyungbuk 760-749, South Korea

Received 14 October 2002; received in revised form 12 July 2003

Abstract

Effects of width and location of a flow disturbing circular plate on nucleate pool boiling heat transfer of water at atmospheric pressure have been investigated experimentally. Through the tests, changes in the degree of intensity of liquid agitation and its effect on heat transfer on a heated tube have been analyzed. According to the results, the plate changes fluid flow around the tube as well as heat transfer coefficients on the tube. It is identified that plate width changes the rate of circulating flow whereas its location changes the growth of active agitating flow. Moreover, flow chugging was observed at the downside of the plate.

1. Introduction

The mechanism of pool boiling heat transfer has been studied for a long time since it is closely related with the designs of more efficient heat exchangers. Recently, it has been widely investigated in nuclear power plants for application to the design of new passive heat removal systems employed in the advanced light water reactors [1,2]. One of the generally adopted geometries for the heat exchangers is tubular type and the orientation of the heat exchanging tubes is usually in vertical direction. Although many researchers have investigated effects of the several design parameters on pool boiling heat transfer for the past several decades [3], researches for a vertical tube are relatively small. Changes in the degree of pool boiling heat transfer closely depend on the heating surface geometry (i.e., wire, plate, or tube). Cornwell and Houston [4] suggested that nucleate boiling on a tube differs considerably from that on a flat plate. The same is true for a wire. Therefore, results for a flat plate and a wire cannot apply to a tube without significant modification. Some previous researches related with the vertical orientation, regardless of the geometry, are as follows:

Jakob [5] recommended four empirical correlations for water boiling at standard atmospheric pressure under free convection condition. He set up the formulas for the horizontal and vertical heating surfaces in wide vessels. According to the results, the horizontal type is more efficient than the vertical type in the low heat flux (q'') region (less than 11.8 kW/m^2) while the opposite is true in the higher heat flux region.

Stralen and Sluyter [6] performed a test to find out boiling curves for platinum wires in the horizontal and vertical orientations at atmospheric pressure. They said that the horizontal type was more effective than the vertical type both in the natural convection and boiling regions. The peak heat flux for the horizontal type is 45% higher in comparison to the corresponding value for the vertical type. The major cause of the reduction in heat transfer for the vertical position is due to the formation of large vapor slugs. The coalesced bubbles are distributed over the entire heating surface for a vertical wire and this behavior differs from that for a horizontal wire, where bubble coalescence is generally restricted to nearby nuclei.

Nishikawa et al. [7] studied changes in the heat flux and the wall superheat (ΔT_{sat}) on a flat plate oriented at an inclination angle (θ) that varied between 0° and 175° from a horizontal, upward-facing position in the water. According to them, boiling heat transfer coefficients are increased with an increase of the inclination angle at the

* Tel.: +82-54-820-5483; fax: +82-54-823-1766.
E-mail address: mgkang@andong.ac.kr (M.-G. Kang).

0017-9310/$ - see front matter © 2003 Elsevier Ltd. All rights reserved.
doi:10.1016/j.ijheatmasstransfer.2003.07.014

Nomenclature

A	heat transfer area	q''	heat flux
D	heating tube diameter	t	time
D_0	diameter of the flow disturbing plate	T_W	tube wall temperature
h_b	boiling heat transfer coefficient	T_{sat}	saturated water temperature
I	supplied current	V	supplied voltage
L	tube length	W_p	width of the flow disturbing plate ($= (D_0 - D)/2$)
LP	height from the tube bottom		
q	input power		

low heat flux region (less than 100 kW/m^2) and orientation effects become negligible as the heat flux on the surface increases more than 100 kW/m^2. The difference in the effect of surface configuration over the whole region of nucleate boiling is presumed as changes in characteristics of bubble behavior and heat transfer mechanisms between low heat fluxes and high heat fluxes. In addition, they explained the heat transfer mechanisms for the low heat fluxes and high heat fluxes as the inclination angle changes. One year later, Lienhard [8] explained the cause of the loss of orientation dependence using the Moissis–Berenson transition [9].

Jung et al. [10] reported a study of nucleate and film boiling heat transfer in R-11 at 1 and 2 bar as a function of surface characterization and orientation. Through the tests of two metal-coated surfaces and a flat copper surface, it was subjected to heat fluxes up to 180 kW/m^2 with surface orientations varying from horizontally facing upward, to vertical, to horizontally facing downward. They suggested results similar to the Nishikawa et al.'s result [7]. For all surfaces investigated, the superheat decreases by 15–25% as the inclination angle changes from 0° to 165° in the relatively low heat flux range (i.e., 10–40 kW/m^2). Beyond this heat flux range, however, the superheat remains constant regardless of the surface orientation.

Fujita et al. [11] performed some more studies about a flat plate. Fujita et al. studied about the combined effects of the inclination angle and the gap size between two plates under the closed side periphery condition. According to them, effects of the inclination angle are closely related with the gap size. The general trend is similar to the Nishikawa et al.'s result [7]. However, decreasing the gap size to be much narrower (0.15 mm for the case) the boiling behavior does not change with the inclination angle. Chang and You [12] investigated effects of the surface orientation from a microporous-enhanced square heater in FC-72. Some years later, Rainey and You [13] added effects of the heater size to Chang and You's results.

Although many authors studied effects of the inclination angle on pool boiling heat transfer along with effects of geometry, pressure, and surface conditions, no detailed studies have been performed for tubes until Chun and Kang [3] studied effects of tube orientation on pool boiling heat transfer in combination with tube surface roughness and the diameter (D). According to Chun and Kang [3], the slope of q'' versus ΔT_{sat} curve of the vertical tube becomes smaller than that of the horizontal tube as the surface roughness decreases.

Recently, Kang [14] carried out an experimental parametric study of a tubular heat exchanger to determine effects of the tube inclination angle on pool boiling heat transfer. Throughout the study for three inclination angles (0°, 45° and 90°) and two values of the surface roughness (15.1 and 60.9 nm), Kang [14] concluded that tube inclination gives much change on pool boiling heat transfer. Moreover, he identified that the result for a tube is much different from the result for a flat plate. The effect of the inclination angle is more strongly observed in the smooth tube and if a tube is properly inclined (45° for the case) enhanced heat transfer is expected in comparison to the horizontal and the vertical positions. Kang [15] performed some more detailed study for the inclination angle with combining the surface roughness into the analysis.

Summarizing the works, it can be said that although effects of an inclination angle on pool boiling heat transfer have been studied for various heating surface geometries (i.e., wire, plate, or tube), the detailed analysis on the heat transfer mechanism itself is very limited. Cornwell and Houston [4] and Kang [14] have executed to analysis the mechanisms affecting heat transfer on a horizontal tube. They observed variations of the local heat transfer coefficient through the tube circumference and suggested mechanisms of sliding bubble [4] and bubble coalescence [14]. Kang [1,14] also analyzed some mechanisms affecting heat transfer on a vertical tube. Kang [1] suggested a new experimental correlation containing the length of the vertical tube length. Corletti and Hochreiter [2] published some experimental results for a very lengthy vertical tube. They investigated pool boiling heat transfer on the tube surface for application to the advanced light water reactor design.

Summarizing the previous researches on heat transfer mechanisms of pool boiling it can be concluded that the

major changes in the heat transfer rate come from the bubble behavior (i.e., generation, coalescence, and movement). According to Kang [1,14] and Corletti and Hochreiter [2] boiling heat transfer on a vertical tube is dependent on the intensity of (1) liquid agitation, (2) bubble coalescence, and (3) the rapid convective flow around the heated tube surface. Liquid agitation enhances heat transfer whereas bubble coalescence and the rapid convective flow decrease heat transfer from the heated surface. Bubble coalescence on a vertical tube is usually observed at the area where the density of active nucleation sites is very high and the intensity of liquid agitation is very weak. To activate more nucleation sites, the heated surface should be manufactured rougher [15] or the value of the heat flux should be higher. To observe bubble coalescence at the lower heat flux, the geometry of the heated surface should be changed (e.g., annular condition) [16]. The rapid convective flow prevents the generation of fully developed bubbles on the tube surface and, hence, decreases the heat transfer rate at the upper region of the longer tubes installed vertically [2]. Therefore, to fully observe the mechanisms of bubble coalescence and/or rapid convective flow specially manufactured surfaces and/or higher heat fluxes are necessary. However, the intensity of liquid agitation can be observed over the full heat flux range and it is very important to explain the increase in heat transfer at the fixed wall superheat.

Therefore, the present study is aimed at the analysis of the intensity of liquid agitation around a vertical tube. For the tests, the normal flow of bubbles around the heated tube will be disturbed by a flow disturbing plate. With changing width and location of the plate variations in the local and average heat transfer coefficients on the tube surface will be obtained. The investigations on the movement of bubbles along the tube surface and its spreading over the water surface will be focused in the study. If the exact mechanism of the intensity of liquid agitation and its variations was identified, it could be extended to the analysis of the critical heat flux, which is usually the main cause of the severe accident in nuclear power plants.

2. Experiments

2.1. Experimental apparatus

A schematic view of the present experimental apparatus and test sections is shown in Fig. 1. The water storage tank (Fig. 1(a)) is made of stainless steel and has a rectangular cross-section (950×1300 mm) and a height of 1400 mm. This tank has a glass view port (1000×1000 mm) which permits viewing of the tubes and photographing. The tank has a double container system. The sizes of the inner tank are $800 \times 1000 \times 1100$ mm (depth $\times$ width $\times$ height). The bottom side of the inner tank is situated at 200 mm above the bottom of the outer tank. Drainage of the inside tank was done by the two passages situated at the bottom side. Outlets of the drain passages are 50 mm above the bottom side of the outer tank to reduce any possible effects of outside fluid on the flow of the inside tank. The inside tank has several flow holes (28 mm in diameter) to allow fluid inflow from the outer tank. To diminish effects of inflow from outside tank, holes are situated at 300 and 800 mm high from the bottom of the inside tank. Although some area around the hole can be affected by the inlet flow, it is not expected that the inflow would change the flow characteristics nearby the heated tube. Four auxiliary heaters (5 kW/heater) were installed at the space between the inside and the outside tank bottoms to boil the water and to maintain the saturated condition. To reduce heat loss to the environment, the left, right, and rear sides of the tank were insulated by glass wool of 50 mm thickness. The up side of the water storage tank is covered with two stainless steel plates to minimize the loss of the water as small as possible while the water boils. Only very small area is opened to the atmosphere to maintain the atmospheric pressure condition. Most of the evaporated vapor condenses on the downward surface of the upside cover and returns to the water surface. Only small amount of the vapor escapes from the water tank and its effect on the pool boiling is negligible. The heat exchanger tubes are simulated by resistance heaters (Fig. 1(b)) made of a very smooth stainless steel tube ($L = 540$ mm and $D = 19.1$ mm). Several rows of resistance wires are arrayed uniformly inside the heated tube to supply power to the tube (Fig. 2). Both sides of the tube are thermally insulated to prevent any possible heat loss through the ends. Moreover, insulation powder was packed into the space between the tube inside wall and the wires (1) to prevent any possible current flowing to the data acquisition system through the thermocouple lines and (2) to heat the outer stainless steel tube uniformly. The surface of the tube was finished through buffing process to have smooth surface. Electric power was supplied through the bottom side of the tube. For the test, 220 V AC was used.

The tube outside was instrumented with five T-type sheathed thermocouples (diameter is 1.5 mm). The thermocouple tip (about 10 mm) was bent at a 90° angle and the bent tip brazed on the tube wall. The locations of the thermocouples are 70, 170, 270, 370, and 470 mm from the heated tube bottom as shown in Fig. 1(b). The water temperatures were measured by the specially manufactured temperature measuring device (Fig. 1(c)) with six sheathed T-type thermocouples and placed vertically at a corner of the inside tank. The thermocouples are brazed on the surface with equal space (i.e., 180 mm) similar to the heated tube. Since the movement of bubbles and liquid is very active, the attachment of

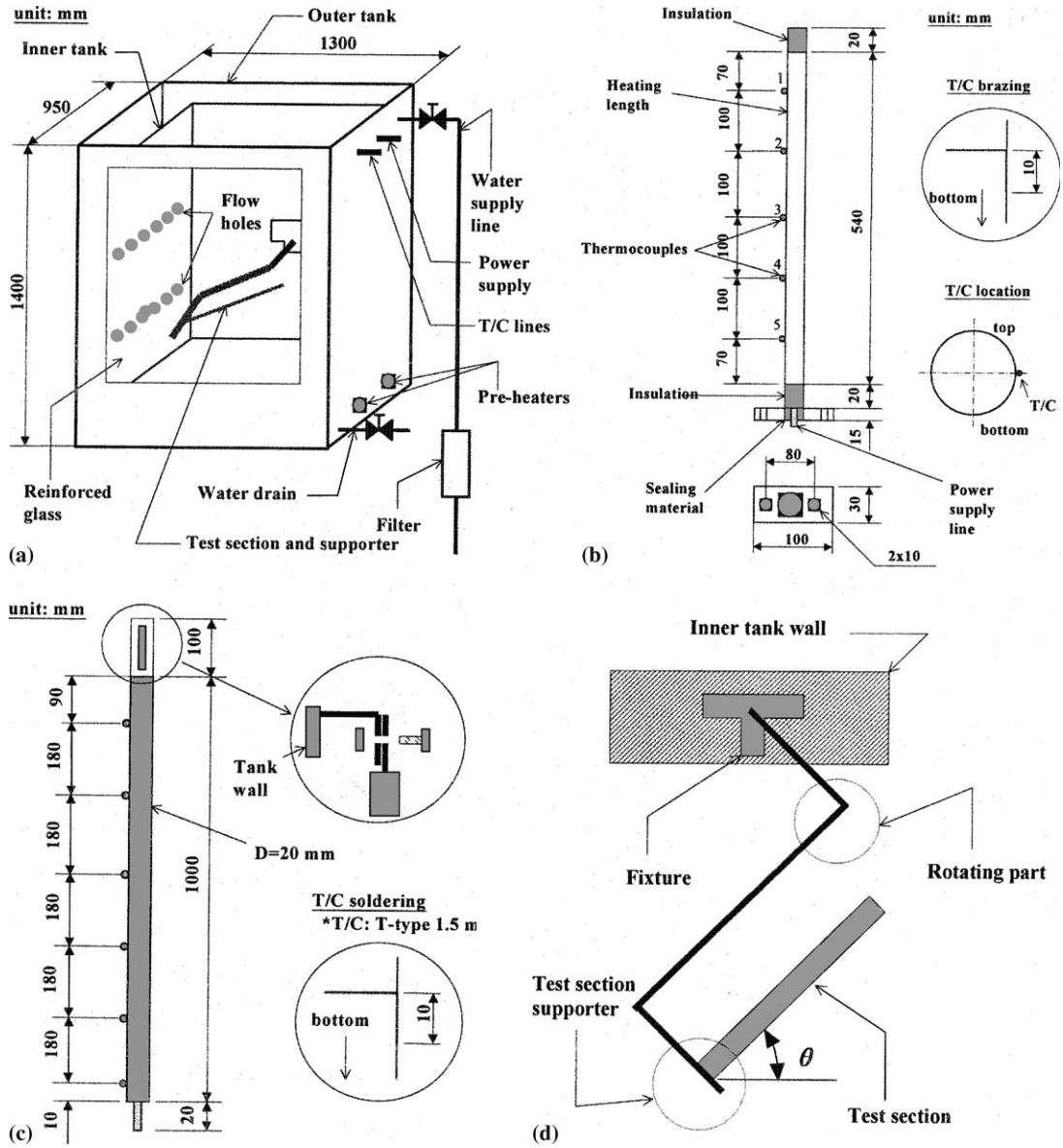

Fig. 1. Schematic diagram of the experimental apparatus.

thermocouples on the tube surface results in no significant change on the fluid movement. At the bottom side of the device a small rod of 10 mm in diameter was attached to fix it to the tank bottom, which has a hole of the same size. The upper side of the device has a hole to fix it to the tank wall with a set of bolt and nut. All thermocouples of the heated tube and the device were calibrated at a saturation value (i.e., 100 °C since all the tests are run at atmospheric pressure condition).

To fix the heated tube onto the right position, a supporter was manufactured as shown in Fig. 1(d). One of the end sides of the supporter is attached at the rear wall of the inside tank and the other free end is connected to the heated tube. The heated tube and the supporter were assembled by the sets of a bolt and a nut. To measure and/or control the supplied voltage and current three power supply systems (each having two channels for reading of voltage and current in digital values) were used. The capacity of each channel is 10 kW.

To observe the intensity of liquid agitation and the flow spreading specially manufactured flow disturbing plates were prepared. The flow disturbing plate is divided into two parts and has an annular shape when

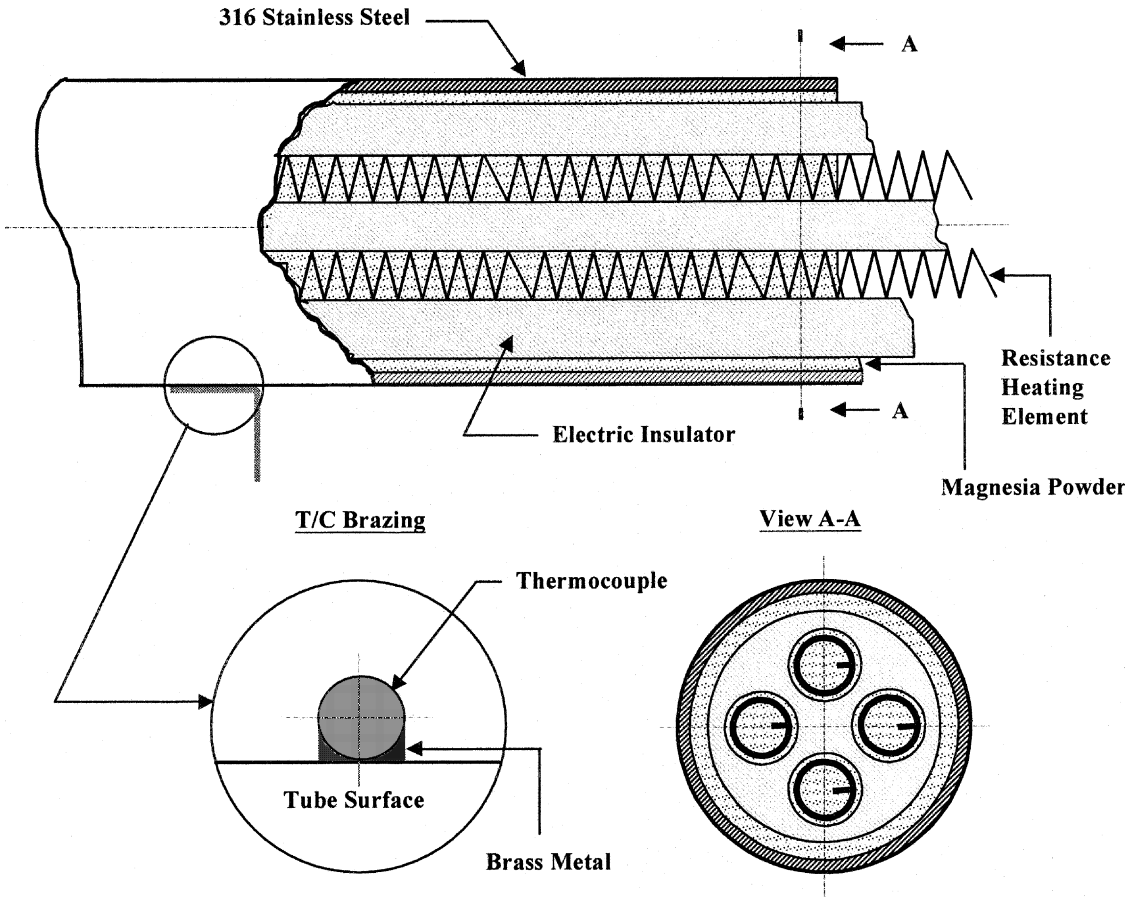

Fig. 2. Cross-sectional view of the heated tube.

fabricated as shown in Fig. 3. The outer diameters (D_0) of the fabricated three plates are 39.1, 59.1, and 79.1 mm, respectively. Therefore, the widths ($W_p = (D_0 - D)/2$) of the plates are 10, 20, and 30 mm, respectively, since the outer diameter of the heated tube is 19.1 mm. For the smooth fabrication of a plate with the heated tube the inside diameter of the plate is manufactured slightly larger (about 0.1 mm) than the tube outer diameter. To prevent sliding of the plate on the tube surface after fabrication, some margin was prepared at the joints. Therefore, the joint points can obtain tight contacts between the plate and the tube. To minimize any possible fin effects due to the attachment of the plate, every contact region (2 or 3 regions of 1–2 mm length) was controlled to maintain point-type contacts. The plates were made of stainless steel and have the thickness of 1 mm. The thickness of the fabricating regions is 0.5 mm to maintain the uniform plate thickness after fabrication. Several screws were used to assemble two parts of the plate into one. Assuming the full contact of the fin inner periphery with the tube surface, the possible maximum increase in heat transfer is less than 1% of the total heat transfer for the single tube without the fin due to the lower fin efficiency (much less than 5%). Therefore, effects of the fin on changes of the heat transfer are very small and can be negligible for the present case of a point type contact.

2.2. Test process

For the tests, the heat exchanging tube is placed vertically at the tube supporter. After the water storage tank is filled with water until the initial water level is at 1200 mm from the outer tank bottom, the water is heated using four pre-heaters at constant power (5 kW/heater). Through the heating process, temperatures of the water were measured. When the water temperature reaches the saturation temperature, the water is then boiled for 30 min to remove the dissolved air. When the water is saturated, there is no temperature gradient through the vertical and horizontal directions. Thereafter, the supply of electricity to the heated tube started. The temperatures of the water and tube surfaces are measured when they are at steady state while controlling

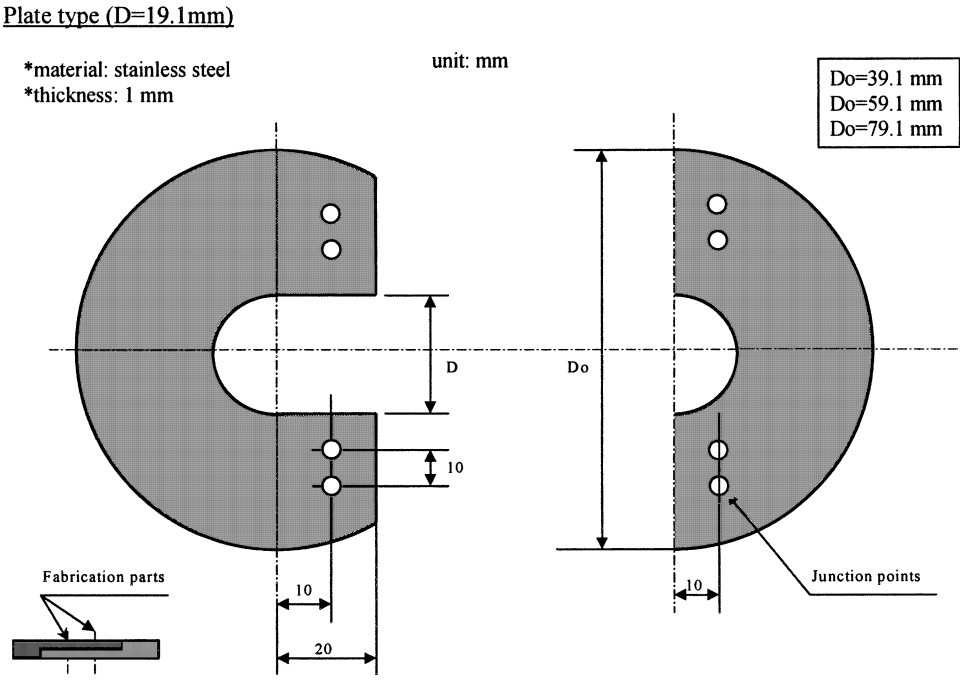

Fig. 3. Schematic of the flow disturbing plate.

the heat flux on the tube surface with input power. In this manner a series of experiments has been performed for various combinations of the width and the location of the flow disturbing plate. Throughout the tests, auxiliary heaters were maintained on condition to certain the water to be saturated.

After a test for the given set of the width and the location is over, the switches to supply electricity to the heaters were turned off and, then, the water was drained. After changing the location or the width of the plate, a new test is started according to the above mentioned test procedure. The test matrix is shown in Table 1. Every experimental data were measured as the heat flux is decreasing. According to Kang [17], no significant hysteresis is observed in the boiling tests for the combination of a smooth stainless steel tube and water like present tests. Therefore, the present results might be applied to the tube as the heat flux increases, too.

The heat flux from the electrically heated tube surface is calculated from the measured values of the input power as follows:

$$q'' = \frac{q}{A} = \frac{VI}{\pi DL} = h_b(T_W - T_{sat}) = h_b \Delta T_{sat} \quad (1)$$

where V and I are the supplied voltage (in volt) and current (in ampere), and D and L are the outside diameter and the length of the heated tube, respectively. T_W and T_{sat} represent the measured temperatures of the tube surface and the saturated water, respectively. The tube surface temperature T_W used in Eq. (1) is the arithmetic average value of the temperatures measured by five thermocouples brazed on the tube surface.

Table 1
Test matrix for the tests

Test no.	Flow disturbing plate	
	Outer diameter, D_0	Location, LP
1	Single tube without the plate	
2	79.1 mm	460 mm, TC1–TC2
3	79.1 mm	360 mm, TC2–TC3
4	79.1 mm	260 mm, TC3–TC4
5	79.1 mm	160 mm, TC4–TC5
6	39.1 mm	460 mm, TC1–TC2
7	59.1 mm	460 mm, TC1–TC2

2.3. Uncertainty of the tests

The error bounds of the voltage and current meters used for the test are ±0.5% of the measured value. Therefore, the calculated power (voltage×current) has ±1.0% error bound. Since the heat flux has the same error bound as the power, the uncertainty in the heat flux is estimated to be ±1.0%. When evaluating the uncertainty of the heat flux, the error of the heat transfer area is not counted since the uncertainties of the tube diameter and the tube length are ±0.1 mm and its effect on the area is negligible.

The measured temperature has uncertainties originated from the thermocouple probe itself, thermocouple brazing, and translation of the measured electric signals to digital values. To evaluate the error bound of a thermocouple probe, three thermocouples brazed on the tube surface were submerged in an isothermal bath containing water. The measured temperatures were compared with the set temperature (80 °C) of the isothermal bath of ±0.01 K accuracy. Since the duration to finish a set of the present test took less than 1 h, the elapsed time to estimate the uncertainty of the thermocouple probes were set as 1 h. Fig. 4 shows the fluctuation bound of the difference between the measured temperatures and the set temperature as a function of time. According to the results, the deviation of the measured values from the set value is within ±0.1 K including the accuracy of the isothermal bath. Since the thermocouples were brazed on the tube surface, the conduction error through the brazing metal must be evaluated. The brazing metal is a kind of brass and the averaged brazing thickness is less than 0.1 mm. The maximum temperature decrease due to this brazing is estimated as 0.15 K. To estimate the total uncertainty of the measured temperatures the translation error of the data acquisition system must be included. The error bound of the system is ±0.05 K. Therefore, the total uncertainty of the measured temperatures is defined by adding the above errors and its value is ±0.3 K.

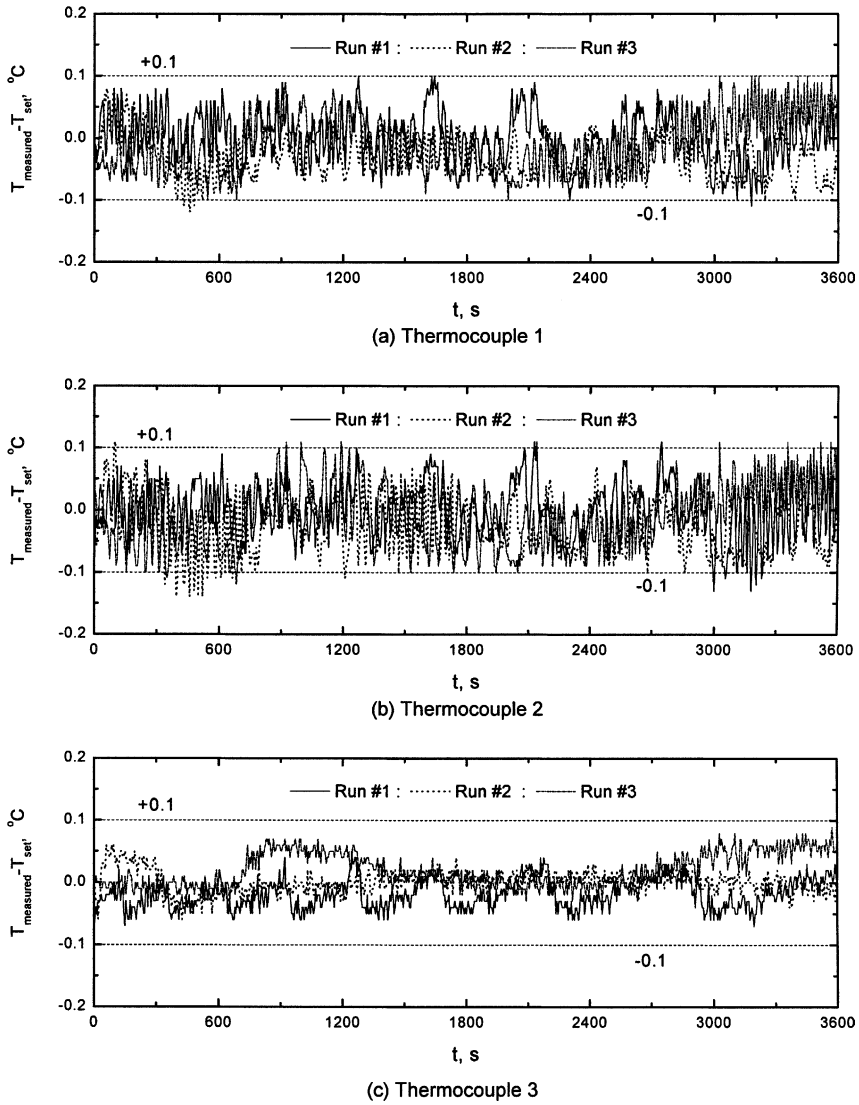

Fig. 4. Comparison of the measured temperatures with the set temperature.

The uncertainty of the calculated heat transfer coefficients (i.e., $h_b = q''/\Delta T_{sat}$) depends on the wall superheat and the heat flux. The maximum possible error is at the highest heat flux (120 kW/m^2 for the case). Since the error bound of the heat flux at its highest value is calculated as ±1.2 kW/m^2 and the uncertainty of the wall superheat is ±0.6 K. The uncertainty of the superheat has been obtained by the equation of the wall superheat (i.e., $\Delta T_{sat} = T_W - T_{sat}$). Therefore, the calculated boiling heat transfer coefficient has its maximum error at $q'' = 120$ kW/m^2 and $\Delta T_{sat} = 10$ K. The value of h_b for the given values of q'' and ΔT_{sat} is 12 kW/m^2 K and the deviation of it, (including errors of the heat flux and the wall superheat) is ±0.5 kW/m^2 K. Therefore, the maximum possible uncertainty of the heat transfer coefficient can be estimated as ±4.2%.

Since the radial heat flux on the tube surface has been assumed uniform, the amount of the axial heat flux should be analyzed to justify its effect on the change of the radial heat flux. The maximum heat flux can be calculated as the difference of the measured local tube wall temperatures has its maximum value. The heat transfer through the axial direction can be calculated using one dimensional conduction equation and the maximum value of the axial heat flux is 0.53 kW/m^2 as the value of the radial heat flux is 100.73 kW/m^2. The ratio of the axial/radial heat fluxes is about 0.5%. The similar ratio can be obtained for the other combinations of the radial heat flux and wall superheat. This ratio is not large enough to change radial heat flux significantly. Therefore, the consideration of the axial heat transfer has been neglected. However, its negligence can be resulted in 0.5% of additional uncertainty on the heat flux.

3. Results and discussion

In order to investigate effects of the location of a flow disturbing plate on pool boiling heat transfer, a plate of 30 mm width was installed at the tube surface. Fig. 5 shows curves of q'' versus ΔT_{sat} and h_b versus q'' as the location of the flow disturbing plate changes from 160 to 460 mm. To clarify effects of the plate on heat transfer, the data were compared with the data of a single tube without the plate. As the plate is located at the tube bottom, decreases in the heat flux were observed at the same tube wall superheat. The slopes of q'' versus ΔT_{sat} and h_b versus q'' curves of the single tube are changed by the presence of the plate. Therefore, it can be supposed that the presence of a flow disturbing plate and its location along the tube can change the mechanisms affecting heat transfer. The major mechanism is liquid agitation due to flow spreading and active bubble movement. The bubbles generated at the tube bottom regions coalesce together with the other bubbles and activate environment liquid while moving toward the water surface. This movement of bubbles changes heat transfer. In a vertical tube condition, some distance is necessary for the flow of bubbles to generate active liquid agitation. If the flow of bubbles developed fully, strong swirling flow of bubbles were observed along the tube. The presence of the plate in front of the flow disturbs the flow of bubbles much before the flow gets fully developed. The dispersed flow has no enough momentum to agitate environment liquid. Therefore, bubbles from the bottom of the plate spread over the plate circumference and, accordingly, the intensity of liquid agitation decreases much. The decrease in the heat flux due to the plate can be observed as the location of the plate

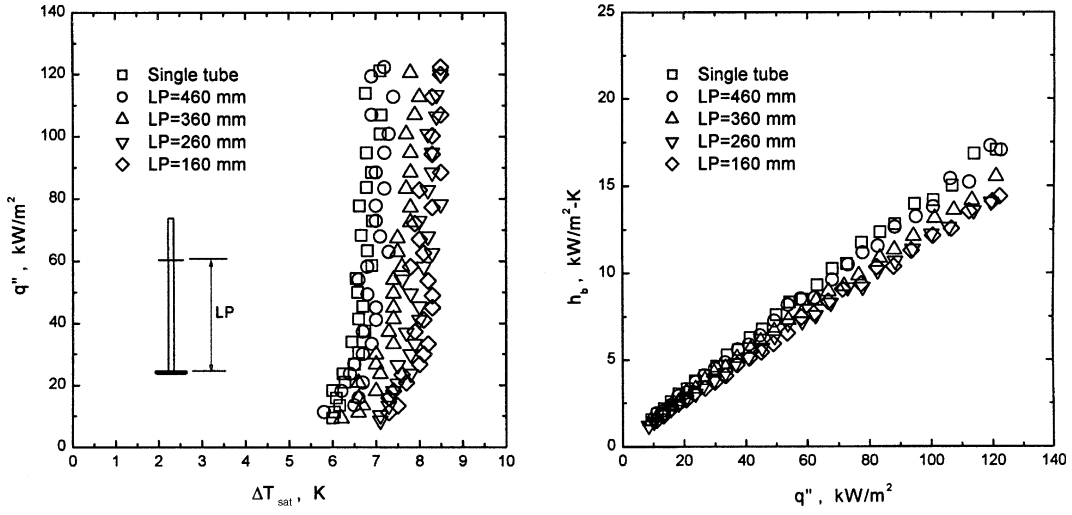

Fig. 5. Changes in heat transfer due to location of the flow disturbing plate ($D_0 = 79.1$ mm).

goes down to LP = 360 mm. As $\Delta T_{sat} = 7$ K, the value of the heat flux for the single tube is 17 times greater than the corresponding values of LP = 160 or 260 mm. However, as the plate is situated at LP = 460 mm the presence of the plate gives no significant change in the heat flux comparing with the single tube without the plate. Therefore, it can be concluded that the minimum distance from the tube bottom is necessary to generate active liquid agitation around the heated tube.

To identify the mechanisms changing heat transfer coefficients boiling on the tube surface has been observed visually. Fig. 6 shows photos of the boiling water on the heated tube surface. Every photos have been taken at LP = 460 mm where the point is between the thermocouple number 1 and 2. The difference among the flow rates of bubbles along the tube can be presumed in the photos with observing boundary of each bubble since the exposure time to take the photos is the same. The individual bubbles in Fig. 6(a) for the single tube are very difficult to distinguish visually one from the others due to the rapid flow rate. However, the bubbles at downstream of the plate in Fig. 6(b) can be distinguished clearly one from the others. Since a bubble is easily distinguished from the other bubbles in the photos of the tube with the plate at LP = 460 mm, it can be said that much slower flow is developed along the tube with the plate comparing to the single tube. However, as the location of the plate is situated at the lower side of the tube it is becoming difficult to identify a bubble from the other bubbles. Comparing photos of Fig. 6(a) and Fig. 6(c)–(e), the flow rate along the tube is fastest at the tube without the plate. The flow rates of bubbles along the

Fig. 6. Photos of pool boiling as the location of the flow disturbing plate ($D_0 = 79.1$ mm) changes. (a) Single tube, (b) LP = 460 mm, (c) LP = 360 mm, (d) LP = 260 mm and (e) LP = 160 mm.

tube might be increased as the location of the plate goes downside of the plate. However, photos of three cases where the plate is between 160 and 380 mm look similar each other. This can be presumed with observing the intensity of the flow of bubbles and clearness of the bubble boundaries. The decrease in the flow rate for three cases with the plate at its lower side is one of the major causes of the decrease in the heat transfer coefficient comparing to the tube without the plate as shown in Fig. 5. Comparing Fig. 6(b) with Fig. 6(c)–(e) one can speculate the relation between the flow rate and the intensity of liquid agitation since much slower flow is supposed in Fig. 6(b). However, the heat transfer coefficient on the tube with the plate at LP = 460 mm is larger than the corresponding values of the other three cases that have the plate at the lower side of the tube (see Fig. 5). Therefore, the existence of the other mechanisms should be considered to explain the non-monotonic trend. One of the mechanisms is related with the spreading of the bubbles through the water surface. In Fig. 6(b), where the plate is installed at 460 mm, bubbles came from the tube lower side are spreading over the area of the disturbing plate. Therefore, it can be explained that the decrease in the intensity of liquid agitation for the tube with the plate at LP = 460 mm is compensated with the bubble spreading over the downstream of the plate.

Local heat transfer coefficients (h_{bc}) on the tube surface at different thermocouple locations were measured to explain the difference in heat transfer coefficients due to the plate location, and the results are shown in Fig. 7. As shown in the figure some discrepancies exist between the trends of the averaged (see Fig. 5) and the local heat transfer coefficients. Observing the experimental results for the single tube shown in Fig. 7(a), no symptom of effective bubble coalescence is identified on the tube surface. If active bubble coalescence exists on the tube surface, there should be sudden decrease in the slope of h_{bc} versus q'' curve [16]. Therefore, it can suggest that the major heat transfer mechanism of the present tests has no relevance with bubble coalescence on the tube surface. At T/C1, the local heat transfer coefficient of the single tube was compared to the corresponding value of the tube with the plate at LP = 460 mm. The value for the tube with the plate is much less than the value for the single tube. There are about 20% difference between two heat transfer coefficients for the tubes with or without the plate at T/C1 and $q'' = 120$ kW/m^2. The major cause for the difference should be liquid agitation as discussed in Fig. 6. Since the rapid flow of bubbles creates strong liquid agitation, the slower flow results in weak liquid agitation. This explanation can be supported by the local heat transfer coefficients for the tubes with the plate at the location lower than LP = 460 mm. As the plate is lower than 460 mm, the local heat transfer coefficient increases at T/C1. As the plate is at the lower side of the tube the flow of bubbles around the upper side of the tube gets faster and results in stronger liquid agitation comparing to the tube with the plate at LP = 460 mm. Comparing the local heat transfer coefficients for the tubes with the plate at 360, 260, and 160 mm, it is identified that there is no significant variation among them. Although the flow rate of bubbles at T/C1 for the tube with the plate at LP = 160 mm is supposed to be faster than the corresponding value for the tube with the plate at LP = 360 mm, no significant changes in local heat transfer coefficients were observed at T/C1. This suggests the importance of the fully developed flow to generate strong liquid agitation.

The averaged heat transfer coefficient, as the plate is at LP = 460 mm, is larger than the heat transfer coefficients as the plate is at the lower side of the tube (see Fig. 5). The cause for the tendency should be observed at the other thermocouple locations. Observing the results at T/C2, the local heat transfer coefficient as the plate is at LP = 460 mm is rapidly increasing as the heat flux increases. The cause is the flow chugging at the lower regime of the plate. If the flow of bubbles flowing upward along the tube surface encounters the disturbing plate, the flow rebounds to downward and this flow mixes actively with the upcoming flow. Then, escapes to the circumference of the plate. The serial process of the bubbles of impact, rebound, mixing to a large bubble slugs, and escape results in the flow chugging under the plate. Thereafter, very active liquid agitation is generated around this area like the pool boiling in an annular space as the tube bottom is closed [16]. The intensity of the flow chugging is magnified, as the flow rate of the bubbles gets bigger. Other important factors contributing to the intensity of liquid agitation is the flow circulation inside the tank. Two major clues observed in this study to explain the circulating flow are (1) the flow of bubbles departed from the upper most region of the tube and (2) the area of bubbles spreading over the water surface. Somewhat clear increases in local heat transfer coefficients of the single tube at T/C3 (Fig. 7(c)) and of the tube with the plate at LP = 460 mm at T/C4 (Fig. 7(d)) are resulted from the circulating flow inside the water tank. The circulating flow can generate liquid agitation at the locations.

To identify the characteristics of the flow spreading and its effects on heat transfer coefficients, the width ($W_p = (D_0 - D)/2$) of the plate has been changed as the plate is at the fixed location of LP = 460 mm. Fig. 8 shows changes in the slopes of q'' versus ΔT_{sat} and h_b versus q'' curves as the values of the width are changing from 10 to 30 mm. According to the results, the heat transfer rate is biggest at the largest plate width ($W_p = 30$ mm). This is caused by the changes in the degree of the flow spreading over the water surface. As the width of the plate gets wider, much stronger circulating flow

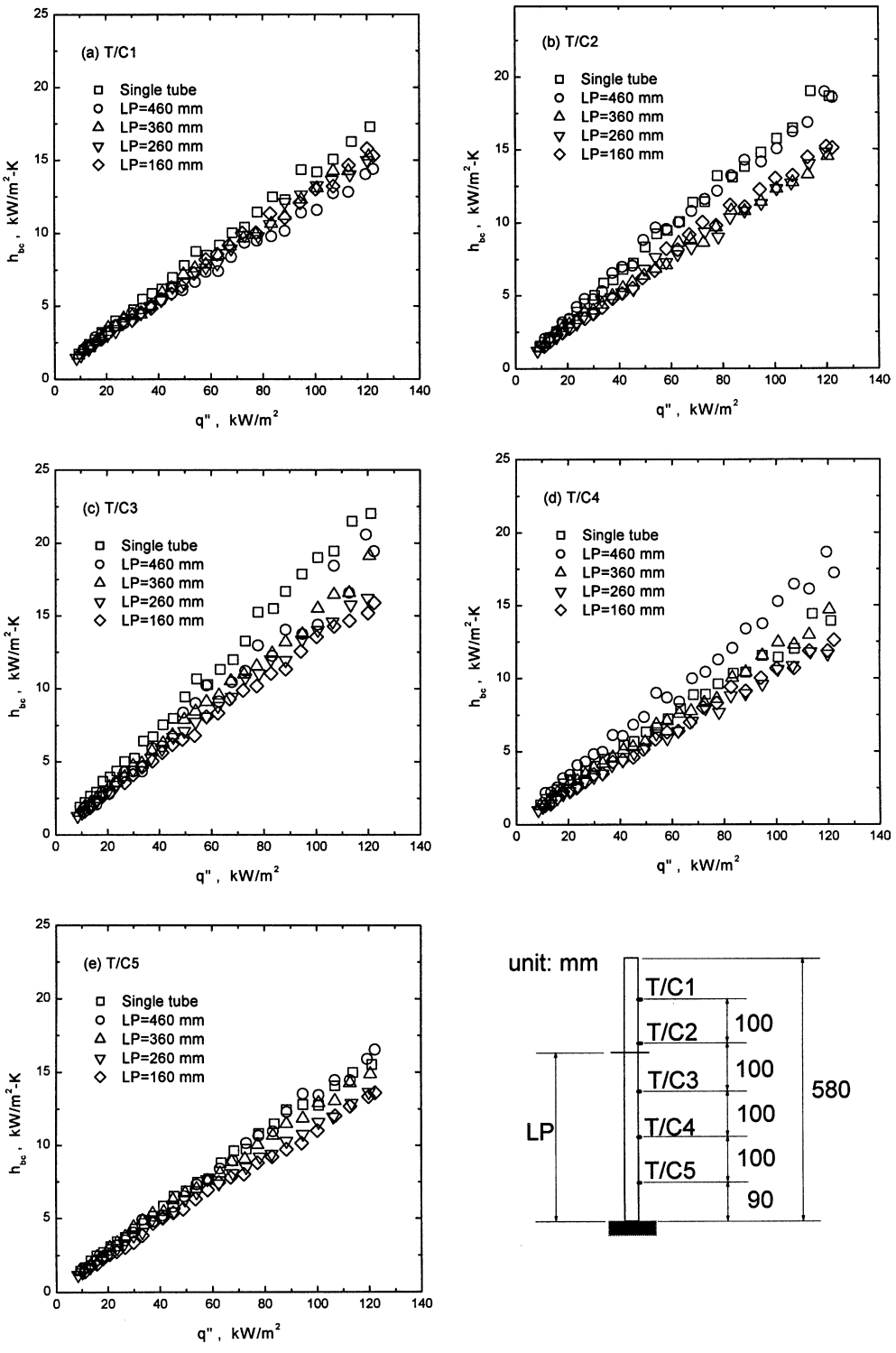

Fig. 7. Changes in local heat transfer coefficients due to location of the flow disturbing plate ($D_0 = 79.1$ mm).

would be resulted in. However, the effect of the flow from the tube lower side on the heat transfer gets increased as the width of the plate decreases. Therefore, the heat transfer coefficient decreases at its first stage as

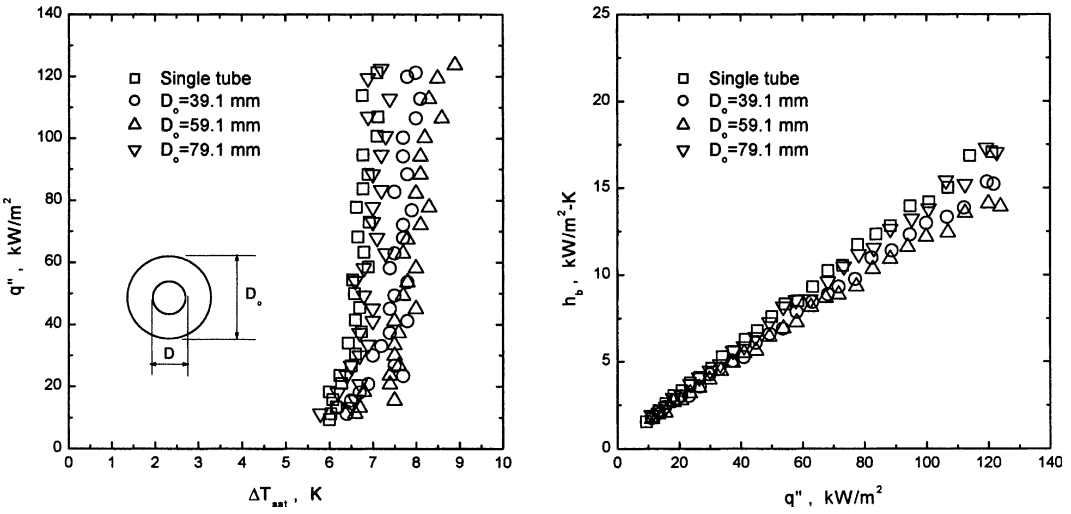

Fig. 8. Changes in heat transfer due to size of the flow disturbing plate (LP = 460 mm).

the plate width decreases. When the width of the plate is between 10 and 20 mm, the threshold of the increase and the decrease in the heat transfer coefficient exists.

Some photos of boiling as the width of the plate is changing are shown in Fig. 9. As the width of the plate is 10 mm (see Fig. 9(b)) the boundary of each bubble at the downstream of the plate gets obscure comparing with those of the wider plates (see Fig. 9(c) and (d)). This suggests that the existence of the faster flow rate and stronger liquid agitation around this region. Therefore, the increase in the local heat transfer coefficient at the downstream of the plate can be expected as $W_p = 10$ mm. When $W_p = 30$ mm the flow of bubbles at the downstream of the plate is spreading widely. This also results in the increase in the heat transfer coefficient due to the circulating flow at the upstream regions of the plate as suggested above. However, as $W_p = 20$ mm neither the intensity of the bubble spreading nor the flow rate of bubbles are increased. Therefore, the heat transfer coefficient at the fixed heat flux has its least value at $D_0 = 59.1$ mm as shown in Fig. 8.

Fig. 10 shows variations in local heat transfer coefficients at the thermocouple locations as the width of the plate changes. At T/C1, the single tube without the plate and the tube with the plate of 10 mm width ($D_0 = 39.1$ mm) have larger heat transfer coefficients comparing to the other two cases with wider plates. The cause is due to liquid agitation created by the faster flow of bubbles around this region. However, at T/C4 location the plate should be wider to have strong liquid agitation (see Fig. 10(d)). As the width of the plate gets narrower the rate of the circulating flow decreases due to the smaller spreading of bubbles at water surface. Comparing the three plate cases with the single tube at T/C4 location, the case of $W_p = 30$ mm ($D_0 = 39.1$ mm) has the biggest heat transfer coefficient whereas the other three cases have the similar values. Therefore, it can be concluded that, the size of the plate should be wider to generate faster circulating flow at the tube lower side. Once a plate is located at LP = 460 mm, it is difficult for the flow to recover the similar intensity of liquid agitation comparing to the cases where the plate is located at the lower side of the tube. Comparing the curves at T/C2 in Fig. 7 with in Fig. 10, the present local heat transfer coefficients are bigger than the local values of the tubes with the plate at lower regions of the tube. This tendency is resulted from the generation of the chugging flow under the plate. If the flow chugging occurs, active liquid agitation is generated at this region, and this results in heat transfer increase. Larger values in the slopes of h_{bc} versus q'' curves are observed at T/C3 for the single tube and at T/C4 for the tube with a plate of 30 mm width. However, this tendency is not observed, as the width of the plate is narrower ($W_p = 10$ or 20 mm) than $W_p =$ 30 mm. Comparing the local heat transfer coefficients at T/C5 as shown in Fig. 10(e), the cases of the single tube and the tube with the wider plate have the values more than 30% bigger than the cases of the narrower width (10 and 20 mm). To magnify the intensity of liquid agitation (1) the flow should be concentrated along the tube like the single tube or (2) it should be spread over wider area like the tube with the plate of 30 mm width.

To clearly identify the changes of the heat transfer coefficient as the heat flux changes, the measured data of the heat transfer coefficients are correlated as a function of the heat flux by using the least square method. The heat transfer coefficients and the heat fluxes satisfy the linear equation form of $h_b = A + Bq''$ where A and B are constants depending on the plate conditions (width and location). The resulting values of the equation are listed

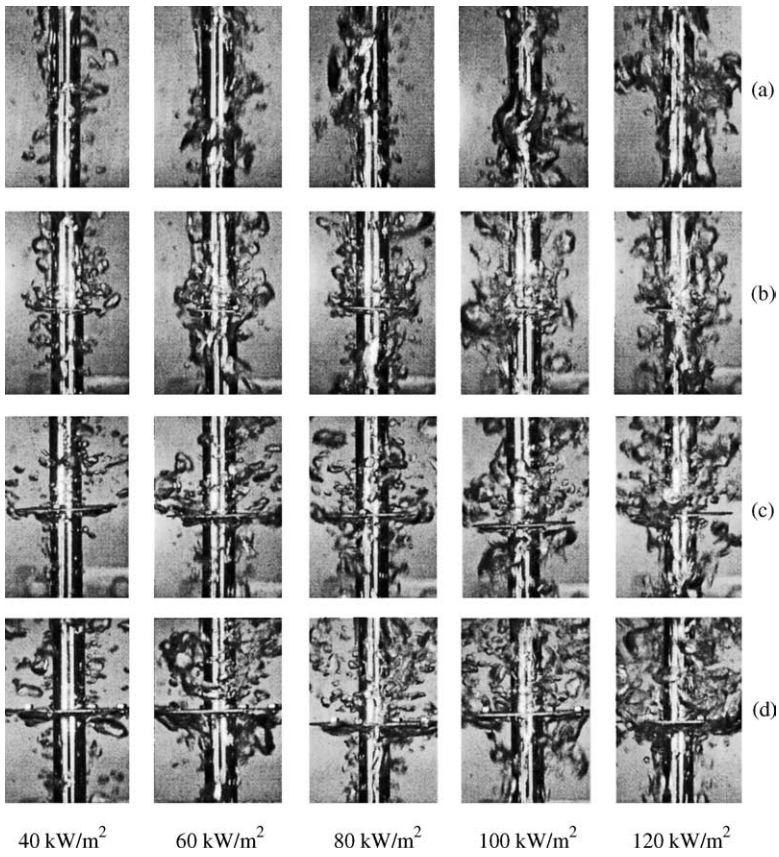

Fig. 9. Photos of pool boiling as the size of the flow disturbing plate changes (LP = 460 mm). (a) Single tube, (b) D_0 = 39.1 mm, (c) D_0 = 59.1 mm and (d) D_0 = 79.1 mm.

in Table 2. To compare the measured and the calculated values, ratios of $h_{b,measured}/h_{b,calculated}$ were calculated and shown in Fig. 11 as a function of heat fluxes. The deviation of the ratios from the exact value is within ±10%. Therefore, it can be said that the correlations predict the measured values well.

Fig. 12 shows the calculated curves of h_b versus W_p and h_b versus LP as a function of the heat fluxes. As the size of the plate width increases from 0 (single tube without the plate) to 20 mm the heat transfer coefficients decrease for the fixed plate location (LP = 460 mm). After then, the heat transfer coefficient increases as the size of the plate width increases from 20 to 30 mm. This tendency is more clearly observed as the heat flux increases since much stronger liquid agitation is expected at the higher heat fluxes. Although the size of the plate is same, the location of it can change the heat transfer coefficient as explained above. The heat transfer coefficient increases as the plate location is situated at the upper side of the tube length for the fixed plate width (D_0 = 79.1 mm). Its effect is much more clearly observed as the heat flux increases.

Summarizing the above-mentioned mechanisms affecting the variations of heat transfer, those can be categorized as two groups of enhancing and decreasing heat transfer, respectively. The mechanisms of enhancing heat transfer on the tube surface are as followings.

(1) Flow spreading: The increase in the area of the flow spreading at downstream of the plate results in faster circulating flow at the upstream regions of the plate. This generates active liquid agitation at the mid-regions of the tube.
(2) Flow chugging: This is observed just at upstream of the plate. As the heat flux increases, many bubbles generated at the lower regions of the tube move upward and merge to the downside of the plate. Then, the bubble slugs come out to the plate circumference along the plate surface. If the size of bubble slugs increases, the impacted bubbles on the plate rebound to the downward. The rebounded bubbles are, then, mixing with the bubbles coming from the downside of the tube. This series of bubble movement results in the chugging flow just at downside of the plate.

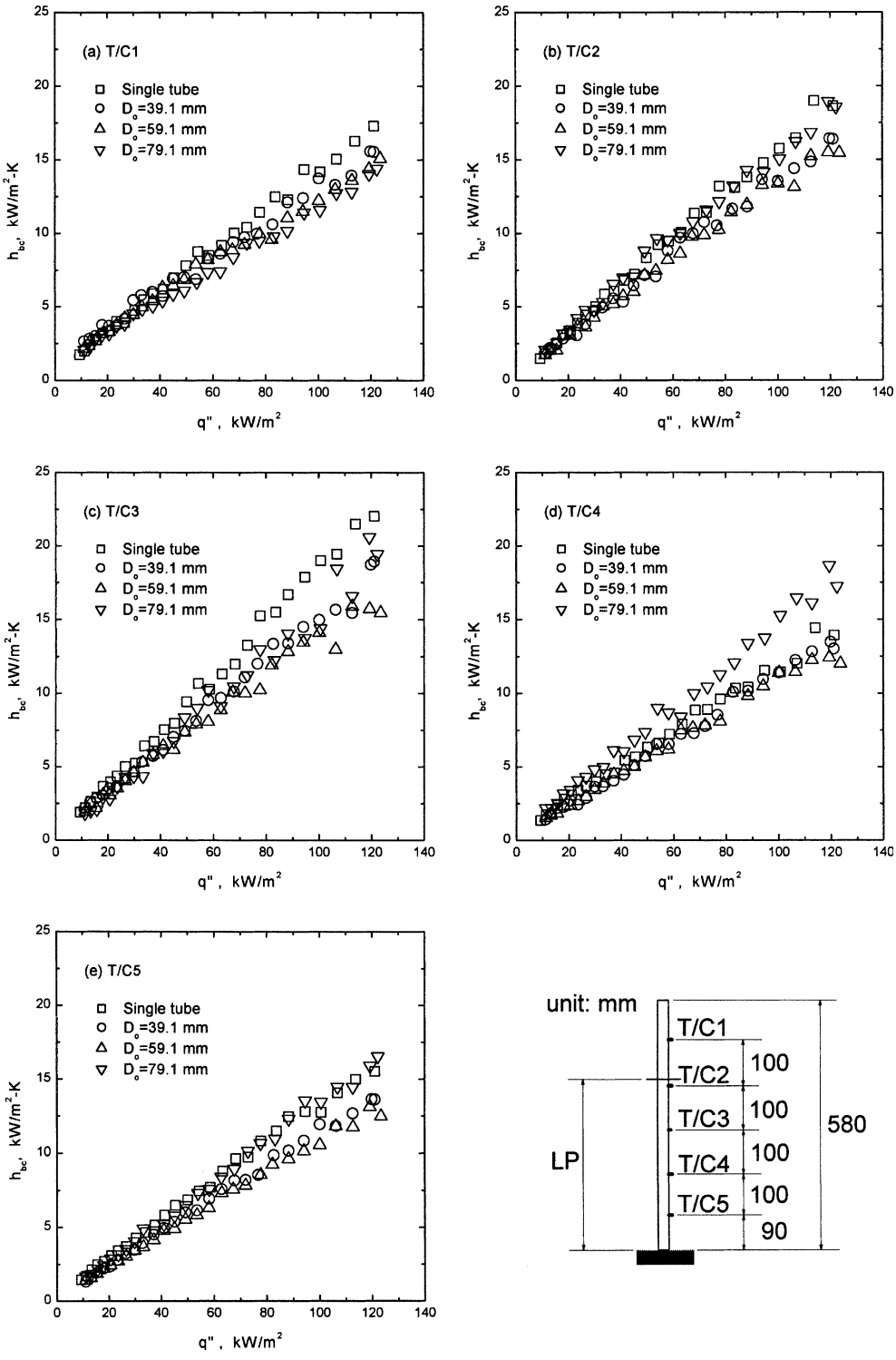

Fig. 10. Changes in local heat transfer coefficients due to size of the flow disturbing plate (LP = 460 mm).

The generation of the chugging flow creates stronger liquid agitation at the downside of the plate.

(3) Flow development length: To get stronger liquid agitation at the upper regions of the tube, enough dis-

Table 2
Results of the curve fitting for the h_b versus q'' data of the 19.1 mm tube diameter (equation: $h_b = A + Bq''$)

Flow disturbing plate		Parameter value		Standard deviation
D_0 (mm)	LP (mm)	A	B	
Single tube		0.40408	0.14065	0.21880
79.1	460	0.35507	0.13708	0.25771
79.1	360	0.45585	0.12366	0.12507
79.1	260	0.36414	0.11656	0.15408
79.1	160	0.30705	0.11684	0.17761
39.1	460	0.45026	0.12304	0.19313
59.1	460	0.60688	0.11397	0.26081

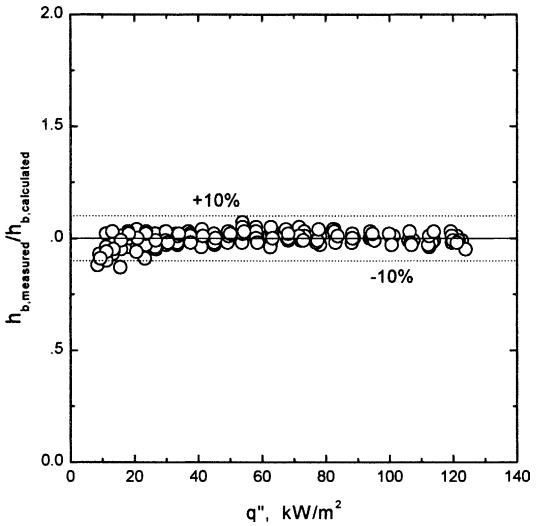

Fig. 11. Comparison between the measured and calculated heat transfer coefficients.

tance is needed for the flow of bubbles to be fully developed. As the flow rate gets faster, stronger liquid agitation at the upper regions of the tube as well as faster circulating flow at the lower regions of the tube can be observed.

The mechanism decreasing heat transfer is the flow stagnation. The flow rate of bubbles gets slower at

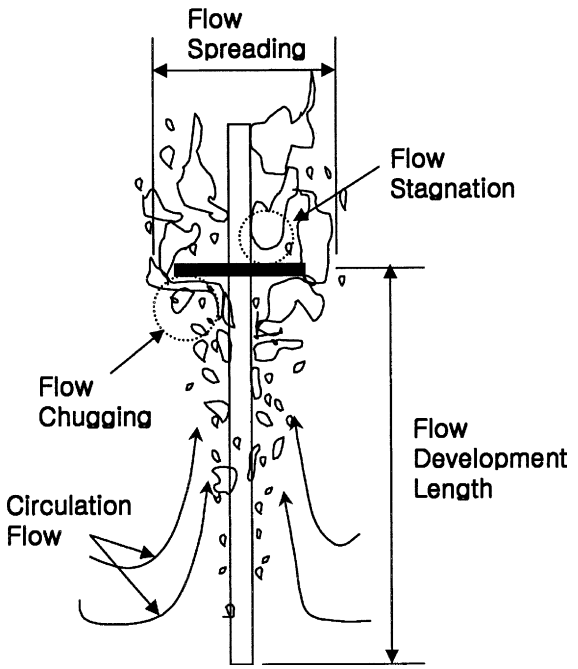

Fig. 13. Schematic view of the mechanisms related with pool boiling heat transfer.

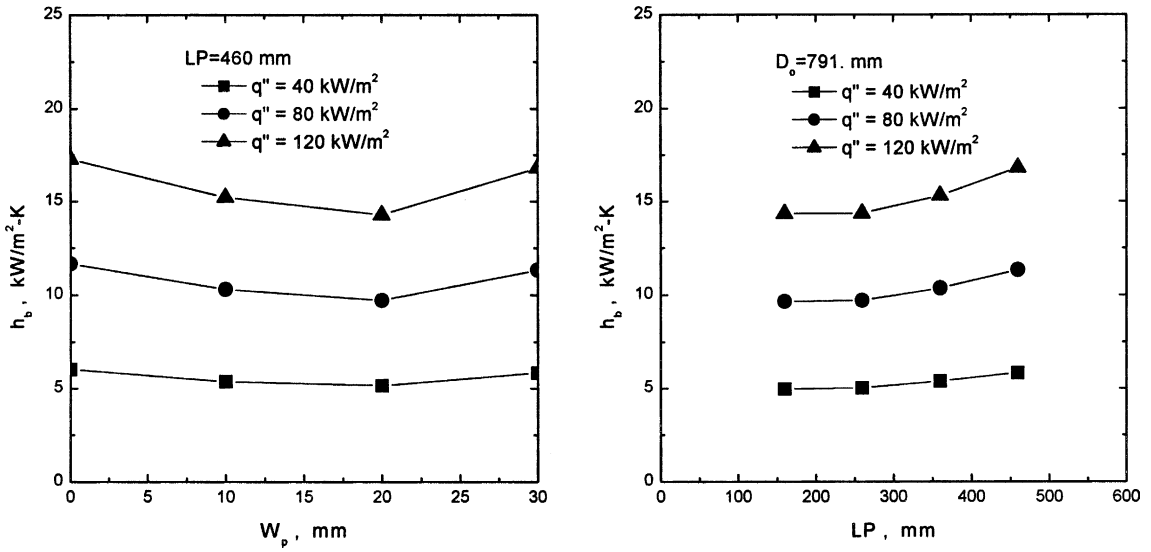

Fig. 12. Changes in heat transfer coefficient as the plate width or location changes.

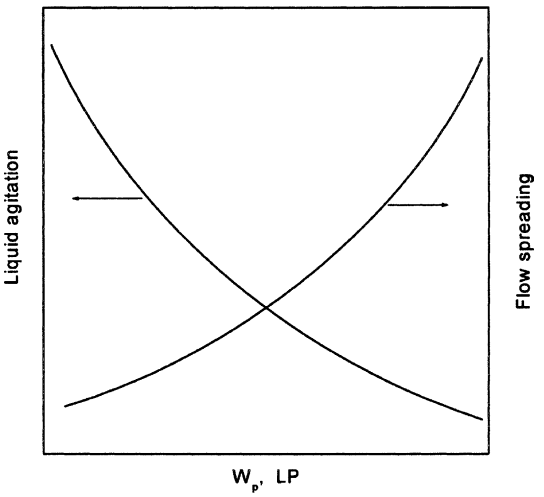

Fig. 14. Changes in the intensity of liquid agitation and flow spreading at the upper most regions of the tube as W_p and/or LP change.

downstream of the plate. Then, the retarded bubbles can be a cause of the flow stagnation. As the flow is stagnant, the intensity of liquid agitation decreases rapidly.

The schematic view of the mechanisms mentioned above is shown in Fig. 13. The changes in the intensity of liquid agitation and flow spreading at the upper most regions of the tube as W_p and/or LP change are shown in Fig. 14. As shown in the figure, the increases in W_p and/or LP decrease the intensity of liquid agitation whereas the decreases in W_p and/or LP increase the area of the flow spreading.

4. Conclusions

To identify effects of the size and location of a flow disturbing plate on pool boiling heat transfer of water at atmospheric pressure, three widths ($W_p = 10$, 20, and 30 mm) and four locations (LP = 160, 260, 360, and 460 mm) of the circular plate have been studied experimentally. In addition, the results were compared with those of the single tube without the plate and some empirical correlations were suggested. The major conclusions of the present study are as followings:

1. The size and/or location of the flow disturbing plate could change the value of the heat transfer coefficient. Moreover, the local heat transfer coefficient and the superheat also can be changed by the adoption of the plate.
2. As the width of the plate is increasing from 0 to 20 mm the heat transfer coefficient decreases. After then, the heat flux increases as the width increases more than 20 mm. This is related with the intensity of the liquid agitation and flow spreading through the inside of the water tank.
3. The averaged heat transfer coefficient increases as the location of the plate ($W_p = 30$ mm) is changed from LP = 160 to 460 mm for the given plate width of 30 mm. Therefore, it can be said that the development of the active liquid agitation is closely related with the flow generated at the tube lower regimes.
4. As the plate is situated at LP = 460 mm where the fully developed bubble flow is observed, the flow chugging and the flow stagnation are observed at the downside and upside of the plate, respectively. The chugging flow increases the heat transfer coefficient and the flow stagnation decreases heat transfer coefficient at the adjacent regions.
5. The measured average heat transfer coefficients and heat fluxes can be correlated as a linear function of $h_b = A + Bq''$ and the empirical correlations can predict the experimental data within ±10% error bound.

Acknowledgements

This work was supported by grant no. R05-2000-000-00309-0 from the Basic Research Program of the Korea Science and Engineering Foundation.

References

[1] M.G. Kang, Experimental investigation of tube length effect on nucleate pool boiling heat transfer, Ann. Nucl. Energy 25 (4–5) (1998) 295–304.
[2] M.M. Corletti, L.E. Hochreiter, Advanced light water reactor passive residual heat removal heat exchanger test, in: Proceedings of the First JSME/ASME Joint International Conference on Nuclear Engineering, Tokyo, Japan, 1991, pp. 381–387.
[3] M.H. Chun, M.G. Kang, Effects of heat exchanger tube parameters on nucleate pool boiling heat transfer, ASME J. Heat Transfer 120 (1998) 468–476.
[4] K. Cornwell, S.D. Houston, Nucleate pool boiling on horizontal tubes: a convection-based correlation, Int. J. Heat Mass Transfer 37 (Suppl. 1) (1994) 303–309.
[5] M. Jakob, G.A. Hawkins, Elements of Heat Transfer, third ed., Wiley International Edition, 1957, pp. 206–210.
[6] S.J.D. Stralen, W.M. Sluyter, Investigations on the critical heat flux of pure liquids and mixtures under various conditions, Int. J. Heat Mass Transfer 12 (1969) 1353–1384.
[7] K. Nishikawa, Y. Fujita, S. Uchida, H. Ohta, Effect of surface configuration on nucleate boiling heat transfer, Int. J. Heat Mass Transfer 27 (9) (1984) 1559–1571.
[8] J.H. Lienhard, On the two regimes on nucleate boiling, ASME J. Heat Transfer 107 (1985) 262–264.
[9] R. Moissis, P.J. Berenson, On the hydrodynamic transition in nucleate boiling, ASME J. Heat Transfer 85 (1963) 221–229.

[10] D.S. Jung, J.E.S. Venant, A.C.M. Sousa, Effects of enhanced surfaces and surface orientations on nucleate and film boiling heat transfer in R-11, Int. J. Heat Mass Transfer 30 (12) (1987) 2627–2639.
[11] Y. Fujita, H. Ohta, S. Uchida, K. Nishikawa, Nucleate boiling heat transfer and critical heat flux in narrow space between rectangular spaces, Int. J. Heat Mass Transfer 31 (1988) 229–239.
[12] J.Y. Chang, S.M. You, Heater orientation effects on pool boiling of microporous-enhanced surfaces in saturated FC-72, ASME J. Heat Transfer 118 (1996) 937–943.
[13] K.N. Rainey, S.M. You, Effects of heater size and orientation on pool boiling heat transfer from microporous coated surfaces, Int. J. Heat Mass Transfer 44 (2001) 2589–2599.
[14] M.G. Kang, Effect of tube inclination on pool boiling heat transfer, ASME J. Heat Transfer 122 (2000) 188–192.
[15] M.G. Kang, Effect of surface roughness on pool boiling heat transfer, Int. J. Heat Mass Transfer 43 (22) (2000) 4073–4085.
[16] M.G. Kang, Y.H. Han, Effects of annular crevices on pool boiling heat transfer, Nucl. Eng. Design 213 (2–3) (2002) 259–271.
[17] M.G. Kang, Hysteresis effects in pool boiling of water, Trans. KSME B 25 (8) (2001) 1037–1045.